Experimental and Numerical Comparison of Currently Available Reaction Mechanisms for Laminar flame speed in Hydrogen/Ammonia Flames

A. ALNASIF [1,2,*], S. ZITOUNI [3], S. MASHRUK [1], P. BREQUIGNY [3] M. KOVALEVA [1]
C. MOUNAIM-ROUSSELLE [3], A. VALERA-MEDINA [1]

[1] College of Physical Sciences and Engineering, Cardiff University, Wales, CF243AA, UK, alnasifah@cardiff.ac.uk
[2] Engineering Technical College of Al-Najaf, Al-Furat Al-Awsat Technical University, Najaf, 31001, Iraq.
[3] Université Orléans, INSA-CVL, EA 4229 – PRISME, F-45072, France .

Abstract: The importance of ammonia as an alternative fuel for mitigating global warming emissions from the environment has become a growing topic in the research community. Due to the viability of ammonia as a hydrogen energy carrier, the molecule has encouraged considerable research towards its utilization as a combustion fuel. To understand the combustion characteristics of ammonia as a prospective fuel in internal combustion engines and gas turbines, the premixed laminar burning velocity of a binary fuel consisting of NH_3-H_2 has been investigated experimentally and numerically. A series of experiments using the spherical expanding flame set-up was employed to measure the laminar burning velocity of a $70NH_3/30H_2$ (%vol) blend of ammonia/hydrogen, at standard temperature and pressure across a wide range of equivalence ratios (0.8 – 1.4). ANSYS CHEMKIN-Pro software was used to perform an extensive numerical modelling analysis, appraising for 36 kinetic reaction mechanisms. Results show how some widely employed kinetic models are not able to accurately predict the Laminar flame speed, especially at leanest conditions. The kinetic mechanism of Duynslaegher et al. (2012) shows the ability to estimate lean conditions with minimal discrepancy and therefore has been identified as the best for estimation of premixed Laminar flame speed in lean conditions. Meanwhile, the kinetic reaction mechanism of Nakamura et al. (2017), demonstrates a good estimation with a small error when the equivalence ratio varies from 1.2 and 1.4.

Keywords: Ammonia, Binary flames, Kinetic modeling, Laminar flame speed, Reaction mechanisms

1. INTRODUCTION

Over the last century, the energy needs of our society have been largely supported by the abundance of cheap hydrocarbon-based fuels, accounting for nearly three-quarters of our global primary energy consumption (H. Ritchie and M. Roser, 2020). Declining indigenous resources coupled with the well-established environmental and ecological adversities resulting from hydrocarbon combustion have helped strive to focus on the study of alternative fuel sources (Riaz et al., 2013). In this regard, ammonia (NH_3) has received a lot of attention lately (Chai et al., 2021a; Valera-Medina et al., 2018), as an efficient zero-carbon energy carrier. NH_3 offers higher gravimetric H_2 content than for example methanol, gasoline, and ethanol (Chatterjee et al., 2021; Valera-Medina et al., 2018) and can be synthesized from fossil fuels, or renewable energy sources coupled with an already mature infrastructure and storage system (Um et al., 2014; Valera-Medina et al., 2018). As such, NH_3 has became a promising alternative fuel, with its utilization demonstrated in high-pressure energy systems such as industrial gas turbines and gas engines (Lhuillier et al., 2021; Valera-Medina et al., 2018, 2017). However, several combustion features of these flames require further understanding.

The Laminar flame speed is a fundamental physiochemical property of a premixed combustible mixture, resulting from the shared influence of mass and thermal diffusion of the reactants and mixture exothermicity (Law, 2006). The laminar flame speed reflects both the combustion process and a characterisation of a given fuel blend, rendering the laminar flame speed a key parameter in helping describe premixed operational instabilities (for example, flash-back, blow-off, and extinction). The laminar flame speed is defined as the velocity a steady one-dimensional adiabatic flame front propagates normal to itself in the doubly infinite domain. This definition renders the laminar flame speed particularly suitable for calculations in one-dimensional simulation which rely on thermodynamic and transport data, and thus by extension convenient in appraising and validating chemical kinetic mechanisms and models (Hu et al., 2015; Law, 2006).

The laminar flame speed of NH_3 known as very low, peaking at slightly rich conditions (equivalence ratio (Φ) of ~ 1.05-1.10), at a value of around 7cm/s (Chai et al., 2021b). Such slow-burning velocities are often associated with low burning efficiencies in engines, potentially yielding poor flame stabilization resulting in local or global extinction. As such, to improve NH_3's combustion characteristics, blending with methane (CH_4) (Henshaw et al., 2005; Pfahl et al., 2000), or H_2 (Lee et al., 2010), as well as oxy-combustion (Li et al., 2015; Takeishi et al., 2015) has been proposed. In this study, a NH_3-H_2 fuel mixture composition of 70%-30% (by vol.%) of has been chosen due to its stable performance in fuelling gas turbine combustors (Mørch et al., 2011; Valera-Medina et al., 2018). The addition of H_2 to NH_3 results in an increase in burning rate (Ichikawa et al., 2015), enhanced the reactivity of the mixture (Chen et al., 2021), and widened flammability limits (Lhuillier et al., 2020). However, the NH_3-H_2 fuel blend has several drawbacks, notably due to higher flame temperatures and abundance of radicals, such as OH, O, and H, potentially causing an increase in NOx formation (Li et al., 2017; Mei et al., 2021b), a detrimental greenhouse gas pollutant.

Recently, significant efforts have been undertaken to establish kinetic models that are able to predict the combustion characteristics of NH_3-H_2 flames, including the commendable efforts to understand ammonia reaction chemistry from various groups worldwide (Glarborg et al., 2018; Klippenstein et al., 2018a; Shrestha et al., 2021, 2018). The optimization process for NH_3-H_2 chemistry entails a specific understanding of the chemistry of each component of fuel and their interactions. Similarly, a chemical kinetic model has also been established by (Mathieu and Petersen, 2015) for ammonia oxidation based on experimental measurements taken inside a shock tube. The resulting mechanism has also been compared with 9 other kinetic mechanisms from the literature (Mathieu and Petersen, 2015). (Glarborg et al., 2018) developed a comprehensive kinetic model including an overview of the most recent data in the kinetic modeling of ammonia combustion. The oxidation kinetic mechanism published by (Shrestha et al., 2018) for pure ammonia and ammonia-hydrogen flames has also received considerable attention, been validated for a number of 0D and 1D energy systems. Li et al. (2019) led also to the development of two reduced models for NH_3-H_2 and NH_3-CH_4-H_2 fuel mixtures respectively. Similarly, many other research groups keep attempting to develop a mechanisms that fully unravels the complexities of using ammonia blends with high accuracy for chemical and numerical studies.

As mentioned above, several numerical and experimental studies have been carried out to understand the combustion characteristics of NH_3-H_2 blends and their applicability in combustion-based systems. The present work deals with this problem by analyzing the Laminar flame speed of a highly stable 70%-30% (vol%) NH_3-H_2 binary fuel blend studied experimentally using a constant-volume spherical vessel, and numerically by modelling Laminar flame speed and comparing 36 currently used chemical kinetic mechanisms. This sheds the light on the performance of these mechanisms and the key kinetic reactions that promote the laminar flame speed in the chemical kinetic environment for various equivalence ratios. The results denote the most accurate mechanisms for various combustion conditions, whilst directing efforts of future works to improve these models for further utilization.

2. METHODOLOGY

2.1. Experimental work

Laminar flame speed measurements were performed using a constant-volume spherical vessel. Details of the rig and post-processing technique can be found in (Galmiche et al., 2012), updated for NH_3 specifications in (Lhuillier et al., 2020) and thus only a brief summary is presented here. The spherical vessel has a nominal internal volume of 4.2 L (ID 200mm), with four orthogonal 70 mm quartz viewing windows with PID temperature control. High-

speed Schlieren imaging of flame propagation was achieved using a CMOS high-speed camera (PHANTOM V1210) set to a suitable fast frame capture rate and facilitating a spatial resolution of ~0.1 mm per pixel. Flame propagation velocities were calculated by edge-detection algorithms written into a bespoke MATLAB script. Reactants were introduced into the chamber using batched thermal mass flow controllers (Brooks 5850S (±1%)). Mass fractions were calculated as a function of initial pressure (P), fuel-air equivalence ratio (Φ), and temperature (T), with mixture concentrations confirmed by partial pressure. Internal fans were used to pre-mix the reactants, and capacitor-discharge ignition was achieved via fine electrodes mounted to 45° to the measurement plane. Experiments were triggered by a simultaneous TTL signal to the ignition system and data acquisition systems after quiescence had been attained. High-purity fuel components of H_2 (>99.95%) and NH_3 (99.95%) and dried compressed air were used to perform the experiments. Measurements were performed at initial conditions of 298 K (± 3K) and 0.1MPa (± 1x10-3Mpa).

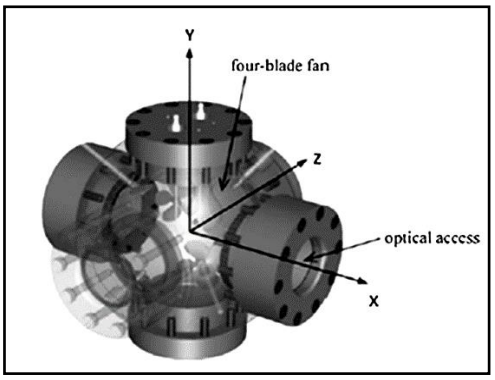

Figure 1: Schematic of Constant Volume Combustion Vessel

To investigate the influence of H_2 on NH_3 flame propagation, spherically expanding flame experiments were conducted for a set molar ratio of H_2 (30%, vol), evaluated across a wide range of equivalence ratio (Φ), to provide a comparison of the change in flame speed from lean to rich conditions. Schlieren measurements were undertaken to evaluate the laminar flame speed relative to the burned side and were experimentally determined by employing the same procedure as in previous studies(Lhuillier et al., 2020; Zitouni et al., 2022). Fig. 2 illustrates an example of images underlining the quality of images taken using the Schlieren optical set-up.

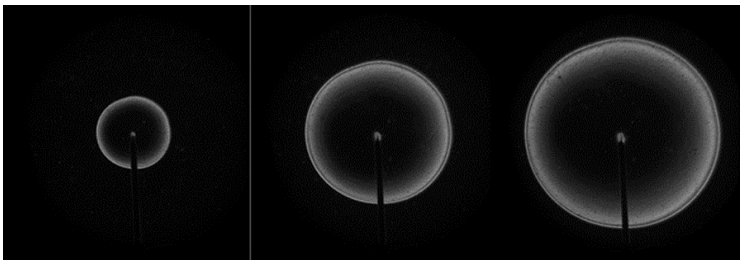

Figure 2: Temporal evolution of a spherically expanding flame using Schlieren imaging

For an outwardly propagating flame, the stretched flame speed (S_n) is expressed as the temporal derivative of the Schlieren flame radius (r_{sch}) as per Equation 1:

$$S_n = \frac{dr_{sch}}{dt} \qquad \text{(Equation 1)}$$

A quasi-steady non-linear association between S_n and stretch, as proposed by (Kelley and Law, 2009) was utilized to obtain an extrapolated unstretched flame speed (S_b), that allows for arbitrary Lewis Number and accounts for deviations in adiabatic and planar assumptions, prominent in flames which are heavily influenced by stretch such as lean H_2-based flames. To obtain an extrapolated unstretched flame speed, a quasi-steady non-linear association between S_n and α is employed (as in Equation 2), re-arranged with the error used for least square regression:

$$\left(\frac{S_n}{S_b}\right)^2 \cdot In\left(\frac{S_n}{S_b}\right)^2 = -\frac{2 \cdot L_b \cdot \alpha}{S_b} \qquad \text{(Equation 2)}$$

Irrespective of the extrapolation methodology employed, to obtain representative values of laminar flame speed, the burned gas expansion must be factored as $U_L = S_b \cdot (\rho_b/\rho_u)$ with ρ_b and ρ_u, burnt and unburnt gases densities calculated using CHEMKIN-Pro.

Substantial efforts are being made to improve the accuracy of reaction mechanisms, which depend on accurate laminar flame speed measurements (Chen, 2015). Uncertain quantification for the present measurements relies upon the methods outlined by (Moffat, 1988), employing a combination of the experimental facility specification and accuracy of the processing techniques chosen. It should be noted that the uncertainty is quantified for the unstretched flame speed (S_b), (and not as opposed to LBV itself), since this is the parameter measured. The total uncertainty estimate is given by Equation 3, where (B_{Sb}) represents the total bias uncertainty, ($t_{M-1,95}$) the student's t value at 95% confidence interval and M-1 degrees of freedom, (σ_{Sb}) is the standard deviation of the repeated experiments, and (M) the number of experimental repeats at each condition; (Brequigny et al., 2019; Lhuillier et al., 2020)

$$U_{Sb} = \sqrt{B_{Sb}^2 + \left(\frac{t_{M-1,95}\sigma_{Su}}{\sqrt{M}}\right)^2} \qquad \text{(Equation 3)}$$

The total bias uncertainty, given by Equation 4, relates changes in S_b with respect to an independent influential variable vi (i.e. temperature, ambient pressure, Φ) and the fixed error linked to that variable -yi-.

$$B_{Sb} = \sqrt{\sum_{i=1}^{n}\left(\frac{\partial S_b(v_i)}{\partial v_i} y_i\right)^2} \qquad \text{(Equation 4)}$$

In order to employ Eqn. 4, the relationships between S_b and each independent variable must be established. The potential changes in S_b from several parameters are calculated as a function of Φ; such as temperature (±3 K), and pressure (±1 x 10^{-3} MPa), with the relationship proposed by (Chen, 2015) employed to evaluate the uncertainty in global Φ. Data modelling employing CHEMKIN-PRO was utilised to estimate these profiles. Uncertainty resulting from the optical system was evaluated from the summated fractional error of both the spatial resolution of the system (±0.05/25mm) and camera (± 1.5/3000fps). Additionally, (Wu et al., 2015) quantified the uncertainty in extrapolation, with corresponding MalinKamid values for data presented in this work falling within the recommended range of -0.05 – 0.15. Accordingly, error bars on all subsequent plots illustrating laminar flame speed measurements are derived from Eqn. 3 & 4, with the error for U_{Su} scaled with respect to the density ratio. A minimum of 5 repeats were conducted per each experimental condition.

2.2. Kinetic modelling.

The analysis of 36 kinetic reaction mechanisms has been performed by ANSYS CHEMKIN-PRO software. A premixed laminar flame-speed calculation model was applied for all reaction mechanisms. The numerical calculations for all model tests were done in a one-dimensional computational domain of length 10 cm, with a maximum grid size of 5000. The adaptive grid control based on solution gradient and curvature was set to 0.02. The grid dependency has been taken into account and the accuracy for all cases was tested and adjusted to give precise results. Table 1 illustrates each mechanism's details regarding the number of reactions and species adopted.

Table 1: Chemical kinetic mechanisms used in the present work

NO.	Kinetic mechanisms reference	No. of Reactions	No. of species	NO.	Kinetic mechanisms reference	No. of Reactions	No. of species
1	(Bertolino et al., 2021)	264	38	19	(U. Mechanism, 2018)	41	20
2	(Mei et al., 2021a)	264	38	20	(Klippenstein et al., 2018b)	211	33
3	(Han et al., 2021)	298	36	21	(Nakamura et al., 2017)	232	33
4	(Mei et al., 2021b)	257	40	22	(Zhang et al., 2017)	251	44
5	(Gotama et al., 2022)	119	26	23	(Lamoureux et al., 2016)	934	123
6	(Shrestha et al., 2021)	1099	125	24	(Xiao et al., 2016)	276	55
7	(Wang et al., 2021)	444	91	25	(Song et al., 2016)	204	32
8	(Zhang et al., 2021)	263	38	26	(Nozari and Karabeyoğlu, 2015)	91	21
9	(Arunthanayothin et al., 2021)	2444	157	27	(Mathieu and Petersen, 2015)	278	54
10	(Stagni et al., 2020)	203	31	28	(Duynslaegher et al., 2012)	80	19
11	(Han et al., 2019b)	177	35	29	(Klippenstein et al., 2011)	202	31
12	(De Persis et al., 2020)	647	103	30	(Zhang et al., 2011)	701	88
13	(Mei et al., 2019)	265	38	31	(Lamoureux et al., 2010)	883	119
14	(Li et al., 2019)	957	128	32	(Konnov, 2009)	1207	127
15	(Okafor et al., 2019)	356	59	33	(Mendiara and Glarborg, 2009)	779	79
16	(Glarborg et al., 2018)	231	39	34	(Tian et al., 2009)	703	84
17	(Shrestha et al., 2018)	1081	124	35	(Dagaut et al., 2008)	250	41
18	(Otomo et al., 2018)	213	32	36	(Smith et al., 2000)	325	53

3. RESULTS AND DISCUSSION

This section addressed the Laminar flame speed modelled by 36 kinetic reaction mechanisms, compared to the experimental results conducted in the present study. To determine the best performing kinetic mechanism for predicting the laminar flame speed of NH_3/H_2 flames at atmospheric conditions, the absolute percentage error (APE) function has been adopted (Armstrong and Collopy, 1992), to calculate the error percentage between the predicted numerical data and experimental results for various equivalence ratios (lean and rich conditions).

3.1. Lean condition flames

Figure 3 shows that Duynslaegher's model provides a good agreement with experimental results with an error equal to approximately 2% followed by Song, Klippenstein, and Nakamura's with around 4% of relative error for each mechanism. For an equivalence ratio of 0.8, Lamoureux et al. (2010) mechanism demonstrated to be the best mechanism in the estimation of laminar flame speed with a minor error of just 1%. On the other side, the relative error for Duynslaegher was recorded at around 6%, as illustrated in Figure 3. When the equivalence ratio is at stoichiometry, Duynslaegher is the best performing mechanism with 0% relative error. Therefore, the Duynslaegher mechanism shows an excellent prediction for the laminar flame speed measurement not only in the stoichiometric conditions but also along with the lean conditions (0.6-1.0).

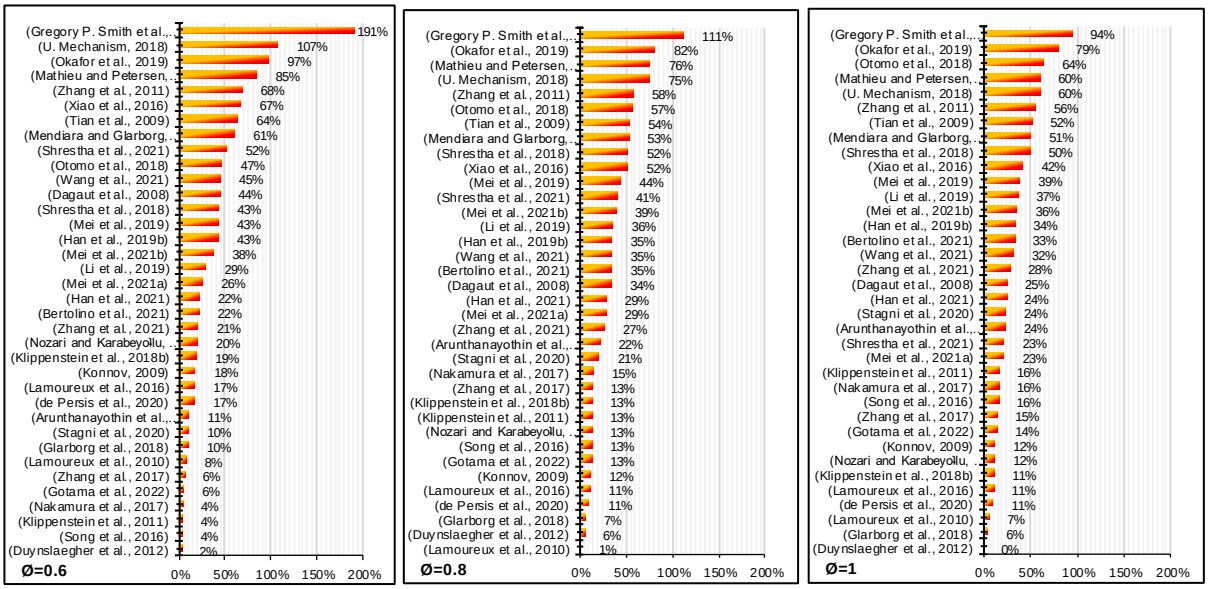

Figure 3: The relative error for 36 kinetic mechanisms for an equivalence ratio range of 0.6-1.0 (lean conditions)

Figure 4 shows the laminar flame speed of the kinetic mechanisms with the lowest error, compared to experimental measurements for the full range of equivalence ratios. As can be seen from figure 4, Glarborg, Lamoureux, and Duynslaegher mechanisms give a good agreement with the experimental measurements in the lean conditions. In spite of there being an underestimation of the laminar flame speed when the equivalence ratio is equal to 0.8, The mechanism of Duynslaegher has a minimum level of discrepancy against the experimental data. The Lamoureux mechanism has good performance at lean conditions and gives only a slight underestimate of laminar flame speed at an equivalence ratio of 0.6, with the error increasing at stoichiometry to give an overestimate of around 7% compared to experimental measurements. The Glarborg kinetic model has a consistent trend line along with the experimental results with an overestimation value for the laminar flame speed between 6% to 10% and for all lean conditions. Finally, the Gotama model shows peak divergence at stoichiometry, but performing fairly well at rich and lean equivalence ratio conditions.

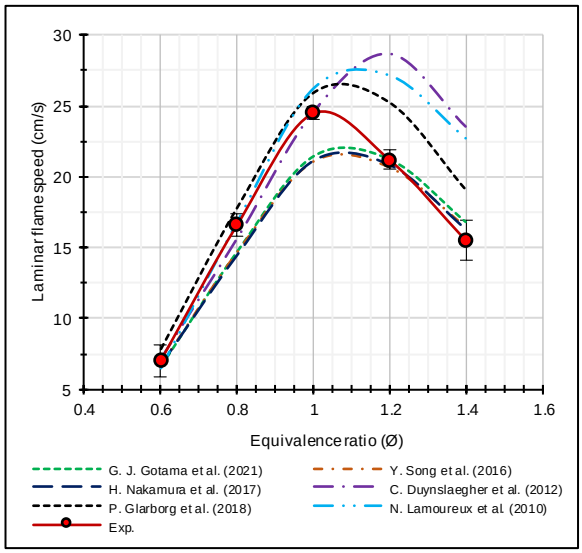

Figure 4: The laminar flame speed for NH_3-H_2 flames predicted by the six best kinetic reaction mechanisms for the full range of equivalence ratios (0.6-1.4).

To analyse the flame speed sensitivity of NH_3-H_2 mixtures, three kinetic reaction mechanisms have been selected (Gotama, Duynslaegher, and Glarborg) based on their performance in lean to stoichiometric equivalence ratios. These mechanisms were chosen because the mechanism of Glarborg slightly overestimates the Laminar flame speed, and the Gotama mechanism slightly underestimates the Laminar flame speed, while the kinetic mechanism of Duynslaegher is in between both, with the lowest error of all.

As shown in Figure 5, each of the bar charts presents the most 10 important reactions in the above selected kinetic mechanisms tested for NH_3-H_2 flames. Since the mechanism of Duynslaegher has a better prediction of the experimental data of laminar flame speed and with a minimum level of error values between 0% to 2% in the full range of the lean condition, the reaction '$NH+H_2O \leftrightarrow HNO+H_2$' recorded a high level of sensitivity and resulted as the second most important kinetic reaction in the promotion of the flame speed in NH_3-H_2 blends in the Duynslaegher reaction model, with sensitivity coefficient values between 0.12 and 0.4 in the lean conditions. It has been also noticed missing this reaction in the database of both Glarborg and Gotama mechanisms. Instead, the previous mechanisms demonstrate the reaction '$NH+O_2 \leftrightarrow HNO+O$' as one of the most three effective reactions in the range of 0.6 and 0.8 of the equivalence ratio.

At an equivalence ratio of 0.6, all three kinetic mechanisms present the chemical reaction '$NH_2+OH \leftrightarrow NH+H_2O$' as a dominant reaction having high sensitivity. Also the sensitivity coefficient values of the mentioned reaction differ from one mechanism to another, where the Glarborg mechanism gives a high level followed by Duynslaegher and Gotama respectively. This is because of the variation of Arrhenius parameters such as rate constant. As shown in Table 2, the kinetic reaction '$NH_2+OH \leftrightarrow NH+H_2O$' estimated by Gotama has large temperature dependence

because of its large value of activation energy, while the same reaction that has been listed in both Duynslaegher and Glarborg mechanism database show low-temperature dependency due to low activation energy. So, the fact that most kinetic reactions are temperature dependent might be the reason behind the discrepancy matter in the prediction of laminar flame speed from one mechanism to another. Also, the difference in which kinetic reactions are included substantially affects the performance of the kinetic mechanism.

At stoichiometric conditions, Duynslaegher mechanismgives an excellent prediction of Laminar flame speed, with an error percentage equal to 0%. As can be seen from figure 5, in addition to the kinetic reaction 'NH+H_2O↔HNO+H_2' mentioned previously, the Duynslaegher reaction model present also another reaction 'NH+OH↔NO+H_2'. This is the case of mechanisms of Gotama and Glarborg, which do not list this kinetic reaction among the ten most important reactions of laminar flame speed. Instead, both mechanisms introduce the kinetic reaction 'NH_2+OH↔HNO+H' as the second important reaction for the promotion of laminar flame speed in stoichiometric conditions. Furthermore, All kinetic models demonstrate a substantial activity of the reaction 'H+O_2↔O+OH', Therefore, this reaction can be considered the dominant kinetic reaction in the laminar flame speed of NH_3-H_2 flames when the blend meets the stoichiometric conditions. The same case can be noticed, which is the sensitivity coefficient values for the same kinetic reaction were varied because of the difference in Arrhenius parameters. As can be shown in Table 2, the reaction 'H+O_2↔O+OH' is a temperature-dependent reaction and its activity is controlled by the activation energy value. Where Dyunslaegher mechanism has higher sensitivity coefficient compared to Gotama and Glarborg kinetic mechanisms. Due to the low activation energy value of this reaction, which is listed in the database of the Duyenslaegher mechanism.

Figure 5: Sensitivity analysis for laminar flame speed of 70NH_3/30H_2 (vo;%) under atmospheric conditions and for three kinetic mechanisms (Gotama et al. 2022, Duynslaegher et al. 2012, and Glarborg et al. 2018) that give a minimum discrepancy value at a lean range of equivalence ratio of 0.6-1.0. Critical reactions for the laminar flame speed are marked in red colour.

Table 2: Key reactions for NH_3-H_2 flames generated from Gotama, Duynslaegher, and Glarborg mechanisms

NO.	Reaction	Gotama et al. (2022)			Duynslaegher et al. (2012)			Glarborg et al. (2018)		
		A	n	E	A	n	E	A	n	E
1	$NH_2+OH\leftrightarrow NH+H_2O$	9.60E+06	2	669	9.00E+07	1.5	-460	3.30E+06	1.90	-217
2	$H+O_2(+M) \leftrightarrow HO_2(+M)$	4.65E+12	0.4	0	1.48E+12	0.6	0	4.70E+12	0.40	0
3	$NH+O_2\leftrightarrow HNO+O$	3.92E+13	0	17885	-	-	-	2.40E+13	0.00	13850

To see the effect of Arrhenius parameters on the laminar flame speed, the Rate of Reaction for the most effective chemical reactions has been plotted at 0.6 of the equivalence ratio. As shown in Figure 6, the reaction rate of $NH_2+OH\leftrightarrow NH+H_2O$, $H+O_2(+M)\leftrightarrow HO_2(+M)$, and $NH+O_2\leftrightarrow HNO+O$ predicted by the Glarborg mechanism were larger than those estimated by both Gotama and Duynslaegher mechanisms and this effect also reflected on the temperature plots for the mentioned mechanisms, where temperature profile estimated by Glarborg model reaction recorded higher value than the other two reaction mechanisms at the position where maximum heat release rate takes place. In addition to that, the peak values of the reaction rate for the mentioned reactions that are estimated by Gotama's mechanism nearly swept to the right compared with peak values for the same reactions calculated by Glarborg and Duynslaegher which are aligned. Further, the reaction rate profiles of '$H+O_2(+M)\leftrightarrow HO_2(+M)$' for all three mechanisms give the same trend, which is in spite of the peak values of this reaction taking place in the reaction zone, this kinetic reaction had the reaction continuous and in progress in the post flame region. Along with that, the reaction rate of the mentioned kinetic reaction predicted by the Duynslaegher mechanism rapidly decreased and reached almost zero around 5.13 cm in comparison to the same kinetic reaction calculated by Gotama and Glarbourg mechanisms that show a higher reaction rate in the same location and decreased gradually to reach nearly zero above 5.3 cm.

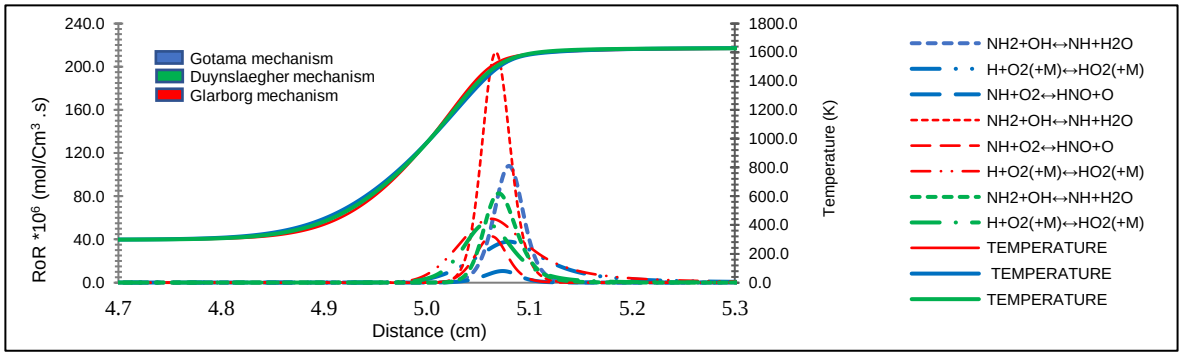

Figure 6: The reaction rate profiles of the key reactions and temperature profiles for NH_3-H_2 flames at Ø= 0.6.

3.2. Rich condition flames

Figure 7 refers to the relative error for laminar flame speed in the rich equivalence ratio range (1.2 and 1.4) As can be seen Nakamura mechanism gives a good estimate of flame speed with error values between 2% and 5% for 1.2 and 1.4 of Ø respectively. Song mechanism has similar performance, with some overestimate at 1.4 equivalence ratio. While Gotama's kinetic model provides an excellent estimate at Ø=1.2, this percentage is increased with increasing equivalence ratio to reach 8% at 1.4. Although Duynslaegher kinetic mechanism demonstrates a good estimation in the lean conditions, Its performance deteriorates in the rich conditions with errors between 26% to 34%, as it is highlighted in Figure 4.

To analyse the origins of these discrepancies between the kinetics mechanisms at rich conditions, Figure 8 shows the sensitivity analysis of the laminar flame speed for rich conditions. When Ø=1.2, the Gotama, and Song kinetic mechanisms present the same most sensitive kinetic reactionsfor the laminar flame speed of NH_3-H_2 with nearly the same estimated sensitivity coefficients. $NH+OH\leftrightarrow HNO+H$ is the kinetic reaction on the top of the list with a higher positive value, while this reaction is in the second order in the Nakamura

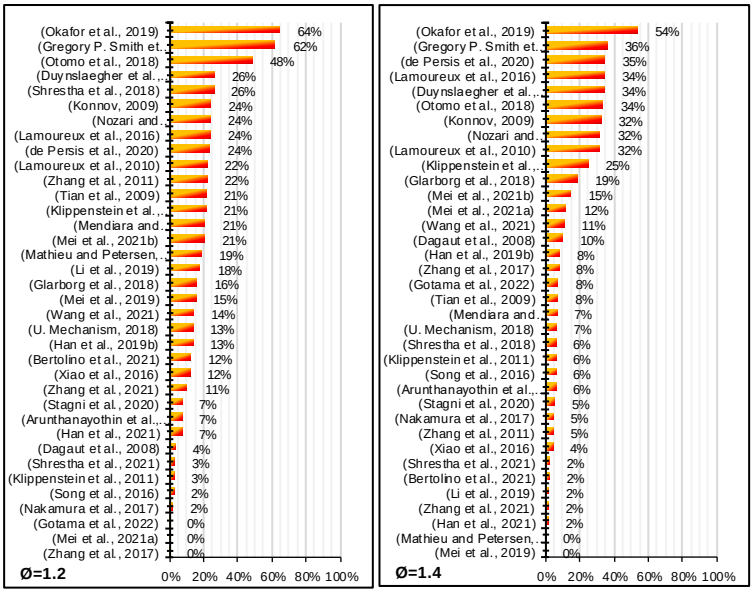

Figure 7: The relative errors for the laminar flame speed predicted by 36 kinetic reaction mechanisms under the rich condition of the equivalence ratio 1.2 and 1.4 respectively.

mechanism. Along with that, the Nakamura mechanism presents three kinetic reactions ($NH_3+H \leftrightarrow NH_2+H_2$, $NH_2+N \leftrightarrow N_2+2H$, and $2NH_2 \leftrightarrow N_2H_2+H_2$) that have not been listed in both Gotama and Song reaction models.

Figure 8: Sensitivity analysis for laminar flame speed of 70NH_3/30H_2 (%vol) under atmospheric conditions and for three kinetic reaction mechanisms (Gotama, Song, and Nakamura) that give a minimum discrepancy value at a rich range of equivalence ratio of 1.2 -1.4. Critical reactions for the laminar flame speed are marked in red colour.

As can be noticed in Fig. 4, the reaction models of Gotama, Song, and Nakamura have all overestimated the laminar flame speed under high rich conditions (Ø=1.4). However, Nakamura kinetic model is the one that has a better prediction for the experimental data with a low discrepancy value. The sensitivity analysis for Nakamura kinetic model shows that $H+O_2 \leftrightarrow O+OH$ presents high positive sensitivity values among other 10 important kinetic reactions followed by $H+O_2(+M) \leftrightarrow HO_2(+M)$. A similar case can be noticed in both Gotama and Song but with different values. Most importantly, the Nakamura mechanism shows the role of both $N+O_2 \leftrightarrow NO+O$ and $H_2+OH \leftrightarrow H+H_2O$ in the promotion of the flame speed in NH_3-H_2 mixtures. While the absence of the effect of the above-mentioned reactions in the other two mechanisms is apparent, both Gotama and Song's kinetic mechanisms show the importance of $NH+H \leftrightarrow N+H_2$ with a sensitivity value between 0.35 and 0.38.

To investigate the reasons behind the discrepancy among the kinetic mechanisms in estimating the flame speed, Figure 9 illustrates the reaction rate for the most important kinetic reactions affecting the laminar flame speed for the Gotama, Song, and Nakamura kinetic mechanisms in terms of temperature and distance for Ø =1.4. The figure shows that the kinetic reaction $H+O_2<=>O+OH$, which is governed by the Gotama mechanism, gives the maximum value of reaction rate compared with Song and Nakamura. Along with that, this type of reaction is highly dependent on temperature, as shown in Table 3. Further, as the Gotama mechanism presents a higher reaction rate for $H+O_2<=>O+OH$ at the reaction zone among other mechanisms, its reaction value decreased sharply when moving away from the reaction zone, this is the case for all reaction mechanisms, and hence goes down underneath Nakamura's reaction rate for the same kinetic reaction. While both reactions $NH+H \leftrightarrow N+H_2$ and $H+O_2(+M) \leftrightarrow HO_2(+M)$ are not temperature-dependent (because they have zero activation energy), the kinetic mechanisms for the last two kinetic reactions have nearly the same values of pre-exponential factor (A) and activation energy (E).

Table 3: Key reactions for the promotion of flame speed of NH_3-H_2 flames at rich conditions and for 3 kinetic mechanisms

NO.	Reaction	Gotama et al. (2022)			Song et al. (2016)			Nakamura et al. (2017)		
		A	n	E	A	n	E	A	n	E
1	H+O2↔O+OH	5.07E+15	-0.5	16126.7	1.00E+14	0	15286	1.04E+14	0	15286.0
2	NH+H↔N+H2	3.01E+13	0	0	3.00E+13	0	0	1.00E+14	0	0
3	H+O2(+M) ↔HO2(+M)	4.65E+12	0.4	0	4.70E+12	0.4	0	4.65E+12	0.4	0

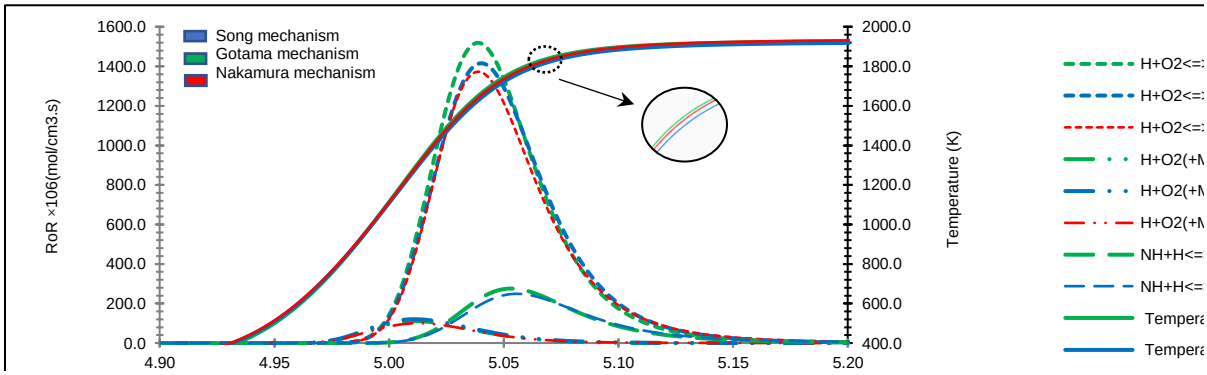

Figure 9: The reaction rate profiles of the key reactions for the laminar flame speed of NH_3-H_2 flames at Ø= 1.4.

Finally, Figure 10 shows the performance of the 36 kinetic reaction mechanisms in the prediction of flame speed of NH_3-H_2 flames and indicates the improvement of the prediction of the kinetic reaction when the mixture takes place in the rich conditions with an error between 15% to 13%. Meanwhile, the flame speed prediction accuracy for the kinetic mechanisms deteriorates at the lean range of the equivalence ratio and reaches a high value of under/overestimation close to 38% at 0.6 (Ø). It also reveals the importance of the oxygenated species, such as O, O_2, OH, and NO in the reaction with ammonia major decomposition products NH_2 and NH.

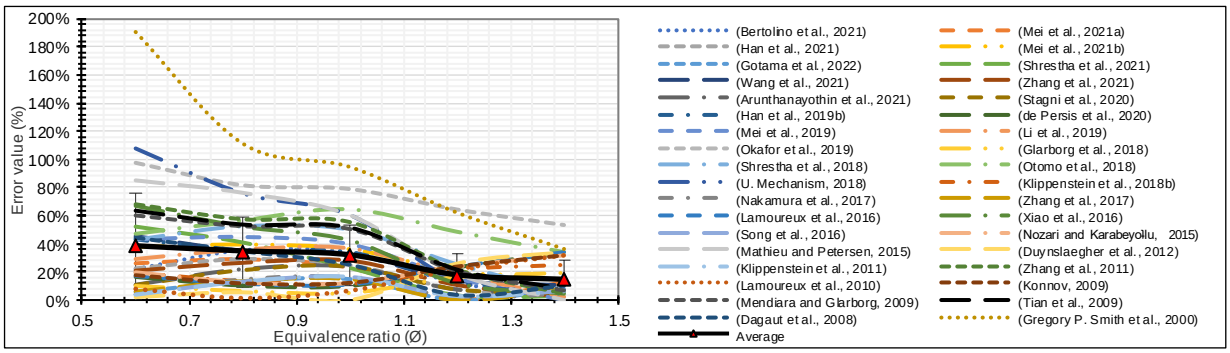

Figure 10: Tthe trend line of prediction error related to the experimental data on the laminar flame speed of NH_3-H_2 flames estimated by all kinetic mechanisms as a function of the equivalence ratio. Symbols denote the average prediction error of 36 kinetic model.

4. CONCLUSION

The present work investigates the laminar flame speed of $70NH_3/30H_2$ (vol%) blended flames for a broad range of the equivalence ratios (0.8-1.4), at atmospheric conditions of pressure and temperature. 36 chemical kinetic mechanisms from the literature were evaluated for their ability to predict Laminar flame speed based on experimental data measured in the present work. The main conclusions are listed as follows:

- The mechanism of Duynslager et al. provides a very good prediction in comparison to the experimental data in the lean range of the equivalence ratio (0.6-1.0) with only low levels of a discrepancy between 0% to 2% were observed. Alongside this comparison, the sensitivity analysis of the laminar flame speed for the Duynslaegher kinetic mechanism reveals the important role of the kinetic reaction '$NH+H_2O↔HNO+H_2$' in the promotion of laminar flame speed at lean conditions.
- The temperature dependency due to the effect of the activation energy of various kinetic reactions was observed to be the reason behind the discrepancy among the kinetic mechanisms, where the activation energy differs in values from one mechanism to another, and this difference affects the reaction rate of each kinetic reaction and hence the laminar flame speed estimation.
- Nakamura kinetic mechanism gives a better prediction of laminar flame speed at rich conditions with low levels of discrepancy (between 2% and 5%). In addition, the Nakamura mechanism shows reactions $NH_3+H↔NH_2+H_2$, $NH_2+N↔N_2+H_2$, and $2NH_2↔N_2H_2+H_2$ at 1.2 of Ø; and $N+O_2↔NO+O$ and $H_2+OH↔H+H_2O$ at 1.4 equivalence ratios as having some of the highest sensitivities to flame speed, compared to the mechanisms, as of Gotama and Song ones, which show different sensitive reactions.

- The estimation accuracy for the 36 kinetic mechanisms varies along with the equivalence ratio. The majority of kinetic mechanisms over or underestimate the laminar flame speed in the lean conditions, especially at 0.6 of equavelance ratio, where the error bars fluctuate close to 38% of the experimental flame speed. However, the performance of these mechanisms improves at rich conditions with a percentage error close to 13% at 1.4 of Ø.

The variation in the estimation of Laminar flame speed from 36 kinetic models has been documented, and only a few of these kinetic mechanisms are able to predict accurately laminar flame speed for a broad range of equivalence ratios. Therefore, modifying and updating these models over time would enable the improvement of future reaction mechanisms for more complex tasks (ie. turbulence industrial modelling.

5. ACKNOWLEDGEMENTS

The authors gratefully acknowledge the support from EPSRC through the project SAFE-AGT Pilot (no. EP/T009314/1) as well as funding from the European Union's Horizon 2020 research and innovation programme under grant agreement No 884157. Furthermore, Ali Alnasif thanks Al-Furat Al-Awsat Technical University (ATU) for the financial support of his PhD studies in the U.K.

6. REFERENCES

Armstrong, J.S., Collopy, F., 1992. Error measures for generalizing about forecasting methods: Empirical comparisons *, International Journal of Forecasting.

Arunthanayothin, S., Stagni, A., Song, Y., Herbinet, O., Faravelli, T., Battin-Leclerc, F., 2021. Ammonia-methane interaction in jet-stirred and flow reactors: An experimental and kinetic modeling study, in: Proceedings of the Combustion Institute. Elsevier Ltd, pp. 345–353. https://doi.org/10.1016/j.proci.2020.07.061

Bertolino, A., Fürst, M., Stagni, A., Frassoldati, A., Pelucchi, M., Cavallotti, C., Faravelli, T., Parente, A., 2021. An evolutionary, data-driven approach for mechanism optimization: theory and application to ammonia combustion. Combustion and Flame 229. https://doi.org/10.1016/j.combustflame.2021.02.012

Brequigny, P., Uesaka, H., Sliti, Z., Segawa, D., Foucher, F., Dayma, G., Mounaïm-Rousselle, C., n.d. Uncertainty in measuring laminar burning velocity from expanding methane-air flames at low pressures.

Chai, W.S., Bao, Y., Jin, P., Tang, G., Zhou, L., 2021a. A review on ammonia, ammonia-hydrogen and ammonia-methane fuels. Renewable and Sustainable Energy Reviews. https://doi.org/10.1016/j.rser.2021.111254

Chai, W.S., Bao, Y., Jin, P., Tang, G., Zhou, L., 2021b. A review on ammonia, ammonia-hydrogen and ammonia-methane fuels. Renewable and Sustainable Energy Reviews. https://doi.org/10.1016/j.rser.2021.111254

Chatterjee, S., Parsapur, R.K., Huang, K.W., 2021. Limitations of Ammonia as a Hydrogen Energy Carrier for the Transportation Sector. ACS Energy Letters 6, 4390–4394. https://doi.org/10.1021/acsenergylett.1c02189

Chen, J., Jiang, X., Qin, X., Huang, Z., 2021. Effect of hydrogen blending on the high temperature auto-ignition of ammonia at elevated pressure. Fuel 287. https://doi.org/10.1016/j.fuel.2020.119563

Chen, Z., 2015. On the accuracy of laminar flame speeds measured from outwardly propagating spherical flames: Methane/air at normal temperature and pressure. Combustion and Flame 162, 2442–2453. https://doi.org/10.1016/j.combustflame.2015.02.012

Dagaut, P., Glarborg, P., Alzueta, M.U., 2008. The oxidation of hydrogen cyanide and related chemistry. Progress in Energy and Combustion Science. https://doi.org/10.1016/j.pecs.2007.02.004

de Persis, S., Pillier, L., Idir, M., Molet, J., Lamoureux, N., Desgroux, P., 2020. NO formation in high pressure premixed flames: Experimental results and validation of a new revised reaction mechanism. Fuel 260. https://doi.org/10.1016/j.fuel.2019.116331

Duynslaegher, C., Contino, F., Vandooren, J., Jeanmart, H., 2012. Modeling of ammonia combustion at low pressure. Combustion and Flame 159, 2799–2805. https://doi.org/10.1016/j.combustflame.2012.06.003

Galmiche, B., Halter, F., Foucher, F., 2012. Effects of high pressure, high temperature and dilution on laminar burning velocities and Markstein lengths of iso-octane/air mixtures. Combustion and Flame 159, 3286–3299. https://doi.org/10.1016/j.combustflame.2012.06.008

Glarborg, P., Miller, J.A., Ruscic, B., Klippenstein, S.J., 2018. Modeling nitrogen chemistry in combustion. Progress in Energy and Combustion Science. https://doi.org/10.1016/j.pecs.2018.01.002

Gotama, G.J., Hayakawa, A., Okafor, E.C., Kanoshima, R., Hayashi, M., Kudo, T., Kobayashi, H., 2022. Measurement of the laminar burning velocity and kinetics study of the importance of the hydrogen recovery mechanism of ammonia/hydrogen/air premixed flames. Combustion and Flame 236. https://doi.org/10.1016/j.combustflame.2021.111753

Gregory P. Smith, David M. Golden, Michael Frenklach, Nigel W. Moriarty, Boris Eiteneer, Mikhail Goldenberg, C. Thomas Bowman, Ronald K. Hanson, Soonho Song, William C. Gardiner, Jr., V.V.L., Zhiwei Qin, 2000. GRI-Mech 3.0 [WWW Document]. http://www.me.berkeley.edu/gri_mech/.

H. Ritchie, M. Roser, 2020. Our World in Data [WWW Document]. Available: https://ourworldindata.org/energy-production-and-changing-energy-sources.

Han, X., Lavadera, L., Konnov, A.A., 2021. An experimental and kinetic modeling study on the laminar burning velocity of NH3+N2O+air flames. Combustion and Flame 228, 13–28. https://doi.org/10.1016/j.combustflame.2021.01.027

Han, X., Wang, Z., Costa, M., Sun, Z., He, Y., Cen, K., 2019. Experimental and kinetic modeling study of laminar burning velocities of NH3/air, NH3/H2/air, NH3/CO/air and NH3/CH4/air premixed flames. Combustion and Flame 206, 214–226. https://doi.org/10.1016/j.combustflame.2019.05.003

Henshaw, P.F., D'Andrea, T., Mann, K.R.C., Ting, D.S.K., 2005. Premixed ammonia-methane-air combustion. Combustion Science and Technology 177, 2151–2170. https://doi.org/10.1080/00102200500240695

Hu, E., Li, X., Meng, X., Chen, Y., Cheng, Y., Xie, Y., Huang, Z., 2015. Laminar flame speeds and ignition delay times of methane-air mixtures at elevated temperatures and pressures. Fuel 158, 1–10. https://doi.org/10.1016/j.fuel.2015.05.010

Ichikawa, A., Hayakawa, A., Kitagawa, Y., Kunkuma Amila Somarathne, K.D., Kudo, T., Kobayashi, H., 2015. Laminar burning velocity and Markstein length of ammonia/hydrogen/air premixed flames at elevated pressures. International Journal of Hydrogen Energy 40, 9570–9578. https://doi.org/10.1016/j.ijhydene.2015.04.024

Kelley, A.P., Law, C.K., 2009. Nonlinear effects in the extraction of laminar flame speeds from expanding spherical flames. Combustion and Flame 156, 1844–1851. https://doi.org/10.1016/j.combustflame.2009.04.004

Klippenstein, S.J., Harding, L.B., Glarborg, P., Miller, J.A., 2011. The role of NNH in NO formation and control. Combustion and Flame 158, 774–789. https://doi.org/10.1016/j.combustflame.2010.12.013

Klippenstein, S.J., Pfeifle, M., Jasper, A.W., Glarborg, P., 2018a. Theory and modeling of relevance to prompt-NO formation at high pressure. Combustion and Flame 195, 3–17. https://doi.org/10.1016/j.combustflame.2018.04.029

Klippenstein, S.J., Pfeifle, M., Jasper, A.W., Glarborg, P., 2018b. Theory and modeling of relevance to prompt-NO formation at high pressure. Combustion and Flame 195, 3–17. https://doi.org/10.1016/j.combustflame.2018.04.029

Konnov, A.A., 2009. Implementation of the NCN pathway of prompt-NO formation in the detailed reaction mechanism. Combustion and Flame 156, 2093–2105. https://doi.org/10.1016/j.combustflame.2009.03.016

Lamoureux, N., Desgroux, P., el Bakali, A., Pauwels, J.F., 2010. Experimental and numerical study of the role of NCN in prompt-NO formation in low-pressure CH4-O2-N2 and C2H2-O2-N2 flames. Combustion and Flame 157, 1929–1941. https://doi.org/10.1016/j.combustflame.2010.03.013

Lamoureux, N., Merhubi, H. el, Pillier, L., de Persis, S., Desgroux, P., 2016. Modeling of NO formation in low pressure premixed flames. Combustion and Flame 163, 557–575. https://doi.org/10.1016/j.combustflame.2015.11.007

Law, C.K., 2006. Combustion physics. Cambridge University Press.

Lee, J.H., Kim, J.H., Park, J.H., Kwon, O.C., 2010. Studies on properties of laminar premixed hydrogen-added ammonia/air flames for hydrogen production. International Journal of Hydrogen Energy 35, 1054–1064. https://doi.org/10.1016/j.ijhydene.2009.11.071

Lhuillier, C., Brequigny, P., Contino, F., Mounaïm-Rousselle, C., 2021. Experimental investigation on ammonia combustion behavior in a spark-ignition engine by means of laminar and turbulent expanding flames, in: Proceedings of the Combustion Institute. Elsevier Ltd, pp. 6671–6678. https://doi.org/10.1016/j.proci.2020.08.058

Lhuillier, C., Brequigny, P., Contino, F., Mounaïm-Rousselle, C., 2020. Experimental study on ammonia/hydrogen/air combustion in spark ignition engine conditions. Fuel 269. https://doi.org/10.1016/j.fuel.2020.117448

Li, J., Huang, H., Kobayashi, N., He, Z., Osaka, Y., Zeng, T., 2015. Numerical study on effect of oxygen content in combustion air on ammonia combustion. Energy 93, 2053–2068. https://doi.org/10.1016/j.energy.2015.10.060

Li, J., Huang, H., Kobayashi, N., Wang, C., Yuan, H., 2017. Numerical study on laminar burning velocity and ignition delay time of ammonia flame with hydrogen addition. Energy 126, 796–809. https://doi.org/10.1016/j.energy.2017.03.085

Li, R., Konnov, A.A., He, G., Qin, F., Zhang, D., 2019. Chemical mechanism development and reduction for combustion of NH3/H2/CH4 mixtures. Fuel 257. https://doi.org/10.1016/j.fuel.2019.116059

Mathieu, O., Petersen, E.L., 2015. Experimental and modeling study on the high-temperature oxidation of Ammonia and related NOx chemistry. Combustion and Flame 162, 554–570. https://doi.org/10.1016/j.combustflame.2014.08.022

Mei, B., Ma, S., Zhang, X., Li, Y., 2021a. Characterizing ammonia and nitric oxide interaction with outwardly propagating spherical flame method. Proceedings of the Combustion Institute 38, 2477–2485. https://doi.org/10.1016/j.proci.2020.07.133

Mei, B., Zhang, J., Shi, X., Xi, Z., Li, Y., 2021b. Enhancement of ammonia combustion with partial fuel cracking strategy: Laminar flame propagation and kinetic modeling investigation of NH3/H2/N2/air mixtures up to 10 atm. Combustion and Flame 231. https://doi.org/10.1016/j.combustflame.2021.111472

Mei, B., Zhang, X., Ma, S., Cui, M., Guo, H., Cao, Z., Li, Y., 2019. Experimental and kinetic modeling investigation on the laminar flame propagation of ammonia under oxygen enrichment and elevated pressure conditions. Combustion and Flame 210, 236–246. https://doi.org/10.1016/j.combustflame.2019.08.033

Mendiara, T., Glarborg, P., 2009. Ammonia chemistry in oxy-fuel combustion of methane. Combustion and Flame 156, 1937–1949. https://doi.org/10.1016/j.combustflame.2009.07.006

Moffat, R.J., 1988. Describing the uncertainties in experimental results. Experimental Thermal and Fluid Science 1, 3–17. https://doi.org/10.1016/0894-1777(88)90043-X

Mørch, C.S., Bjerre, A., Gøttrup, M.P., Sorenson, S.C., Schramm, J., 2011. Ammonia/hydrogen mixtures in an SI-engine: Engine performance and analysis of a proposed fuel system. Fuel 90, 854–864. https://doi.org/10.1016/j.fuel.2010.09.042

Nakamura, H., Hasegawa, S., Tezuka, T., 2017. Kinetic modeling of ammonia/air weak flames in a micro flow reactor with a controlled temperature profile. Combustion and Flame 185, 16–27. https://doi.org/10.1016/j.combustflame.2017.06.021

Nozari, H., Karabeyoğlu, A., 2015. Numerical study of combustion characteristics of ammonia as a renewable fuel and establishment of reduced reaction mechanisms. Fuel 159, 223–233. https://doi.org/10.1016/j.fuel.2015.06.075

Okafor, E.C., Naito, Y., Colson, S., Ichikawa, A., Kudo, T., Hayakawa, A., Kobayashi, H., 2019. Measurement and modelling of the laminar burning velocity of methane-ammonia-air flames at high pressures using a reduced reaction mechanism. Combustion and Flame 204, 162–175. https://doi.org/10.1016/j.combustflame.2019.03.008

Otomo, J., Koshi, M., Mitsumori, T., Iwasaki, H., Yamada, K., 2018. Chemical kinetic modeling of ammonia oxidation with improved reaction mechanism for ammonia/air and ammonia/hydrogen/air combustion. International Journal of Hydrogen Energy 43, 3004–3014. https://doi.org/10.1016/j.ijhydene.2017.12.066

Pfahl, U.J., Ross, M.C., Shepherd, J.E., Pasamehmetoglu, K.O., Unal, C., 2000. Flammability Limits, Ignition Energy, and Flame Speeds in H 2-CH 4-NH 3-N 2 O-O 2-N 2 Mixtures.

Riaz, A., Zahedi, G., Klemeš, J.J., 2013. A review of cleaner production methods for the manufacture of methanol. Journal of Cleaner Production. https://doi.org/10.1016/j.jclepro.2013.06.017

Shrestha, K.P., Lhuillier, C., Barbosa, A.A., Brequigny, P., Contino, F., Mounaïm-Rousselle, C., Seidel, L., Mauss, F., 2021. An experimental and modeling study of ammonia with enriched oxygen content and ammonia/hydrogen laminar flame speed at elevated pressure and temperature. Proceedings of the Combustion Institute 38, 2163–2174. https://doi.org/10.1016/j.proci.2020.06.197

Shrestha, K.P., Seidel, L., Zeuch, T., Mauss, F., 2018. Detailed Kinetic Mechanism for the Oxidation of Ammonia Including the Formation and Reduction of Nitrogen Oxides. Energy and Fuels 32, 10202–10217. https://doi.org/10.1021/acs.energyfuels.8b01056

Song, Y., Hashemi, H., Christensen, J.M., Zou, C., Marshall, P., Glarborg, P., 2016. Ammonia oxidation at high pressure and intermediate temperatures. Fuel 181, 358–365. https://doi.org/10.1016/j.fuel.2016.04.100

Stagni, A., Cavallotti, C., Arunthanayothin, S., Song, Y., Herbinet, O., Battin-Leclerc, F., Faravelli, T., 2020. An experimental, theoretical and kinetic-modeling study of the gas-phase oxidation of ammonia. Reaction Chemistry and Engineering 5, 696–711. https://doi.org/10.1039/c9re00429g

TAKEISHI, H., HAYASHI, J., KONO, S., ARITA, W., IINO, K., AKAMATSU, F., 2015. Characteristics of ammonia/N2/O2 laminar flame in oxygen-enriched air condition. Transactions of the JSME (in Japanese) 81, 14-00423-14–00423. https://doi.org/10.1299/transjsme.14-00423

Tian, Z., Li, Y., Zhang, L., Glarborg, P., Qi, F., 2009. An experimental and kinetic modeling study of premixed NH3/CH4/O2/Ar flames at low pressure. Combustion and Flame 156, 1413–1426. https://doi.org/10.1016/j.combustflame.2009.03.005

U. Mechanism, 2018. Chemical-kinetic mechanisms for combustion applications [WWW Document]. mechanical and aerospace engineering (combustion research), University of California at San Diego.

Um, D.H., Kim, T.Y., Kwon, O.C., 2014. Power and hydrogen production from ammonia in a micro-thermophotovoltaic device integrated with a micro-reformer. Energy 73, 531–542. https://doi.org/10.1016/j.energy.2014.06.053

Valera-Medina, A., Pugh, D.G., Marsh, P., Bulat, G., Bowen, P., 2017. Preliminary study on lean premixed combustion of ammonia-hydrogen for swirling gas turbine combustors. International Journal of Hydrogen Energy 42, 24495–24503. https://doi.org/10.1016/j.ijhydene.2017.08.028

Valera-Medina, A., Xiao, H., Owen-Jones, M., David, W.I.F., Bowen, P.J., 2018. Ammonia for power. Progress in Energy and Combustion Science. https://doi.org/10.1016/j.pecs.2018.07.001

Wang, Z., Han, X., He, Y., Zhu, R., Zhu, Y., Zhou, Z., Cen, K., 2021. Experimental and kinetic study on the laminar burning velocities of NH3 mixing with CH3OH and C2H5OH in premixed flames. Combustion and Flame 229. https://doi.org/10.1016/j.combustflame.2021.02.038

Wu, F., Liang, W., Chen, Z., Ju, Y., Law, C.K., 2015. Uncertainty in stretch extrapolation of laminar flame speed from expanding spherical flames. Proceedings of the Combustion Institute 35, 663–670. https://doi.org/10.1016/j.proci.2014.05.065

Xiao, H., Howard, M., Valera-Medina, A., Dooley, S., Bowen, P.J., 2016. Study on Reduced Chemical Mechanisms of Ammonia/Methane Combustion under Gas Turbine Conditions. Energy and Fuels 30, 8701–8710. https://doi.org/10.1021/acs.energyfuels.6b01556

Zhang, K., Li, Y., Yuan, T., Cai, J., Glarborg, P., Qi, F., 2011. An experimental and kinetic modeling study of premixed nitromethane flames at low pressure. Proceedings of the Combustion Institute 33, 407–414. https://doi.org/10.1016/j.proci.2010.06.002

Zhang, X., Moosakutty, S.P., Rajan, R.P., Younes, M., Sarathy, S.M., 2021. Combustion chemistry of ammonia/hydrogen mixtures: Jet-stirred reactor measurements and comprehensive kinetic modeling. Combustion and Flame 234. https://doi.org/10.1016/j.combustflame.2021.111653

Zhang, Y., Mathieu, O., Petersen, E.L., Bourque, G., Curran, H.J., 2017. Assessing the predictions of a NOx kinetic mechanism on recent hydrogen and syngas experimental data. Combustion and Flame 182, 122–141. https://doi.org/10.1016/j.combustflame.2017.03.019

Zitouni, S., Pugh, D., Crayford, A., Bowen, P.J., Runyon, J., 2022. Lewis number effects on lean premixed combustion characteristics of multi-component fuel blends. Combustion and Flame 238. https://doi.org/10.1016/j.combustflame.2021.111932